The Changes of UV-B Radiation at the Surface due to Stratospheric Aerosols

Jai-Ho Oh, Joon-Hee Jung, and Jeong-Woo Kim

Department of Astronomy and Atmospheric Sciences, Yonsei University, Seoul, Korea

(Manuscript received 16 October 1993)

성층권 에어로졸에 의한 지표면 UV-B 복사량 변동

오재호 · 정준희 · 김정우

연세대학교 천문대기과학과

(1993년 10월 16일 접수)

요 약

대기 가열율과 복사속의 연직 분포를 계산하기 위하여 two-stream/delta-Eddington 근사법을 이용한 복사전달모형이 개발되었다. 이 모형의 결과를 ICRCCM의 결과와 비교하므로써 모형의 완성도를 평가하였다. 이 모형은 정확성 뿐 아니라 경제적인 면에서도 태양복사를 계산하는데 적합한 것으로 증명되었다.

대기 꼭대기에서의 복사속과 지표에서의 복사속 간의 관계를 비교하므로써 자외선 B 영역(UV-B: 280-320nm)의 특징들이 검토되었다. 이 영역에서는 강한 오존 흡수가 있어 UV-B의 관계가 2차 함수로 나타난다. 또한, 성층권 오존 감소와 화산 폭발로 기인한 성층권 에어로졸 안개가 UV-B 복사에 미치는 영향을 다양한 태양의 천정각에서 조사했다. 태양의 천정각이 증가함에 따라 지표 UV-B도 증가하였다. 성층권 에어로졸은 후방 산란을 통해 행성 반사도를 증가시켰다. 행성 반사도는 에어로졸 효과로 인해 태양의 천정각이 증가함에 따라 증가한다. 그러나, 행성 반사도의 변화가 태양의 천정각 변화에 따라 민감하게 나타나지는 않는다. 이것은 태양의 천정각이 클 때 에어로졸의 산란 효과가 상대적으로 긴 복사경로에서 포화되었기 때문일 것이다.

끝으로, 화산 폭발에서 비롯된 성층권 에어로졸이 지표 UV-B 복사 강도에 미치는 지역적 영향이 추정되었다. 고위도에서는 에어로졸의 광자 포획(photon trap)이나 일몰 효과로 복사 강도가 증가하는 반면 저위도에서는 감소한다. 고위도에서 에어로졸의 산란과 오존 흡수는 지표 UV-B 복사에 대하여 큰 영향을 미치며 서로 상반된 효과를 가지고 있다. 이러한 상쇄의 결과로 UV-B 복사의 최대 증가는 봄 기간 중에 양 반구 모두 중위도에서 나타난다.

Abstract

A radiative transfer model with two-stream/delta-Eddington approximation has been developed to calculate the vertical distributions of atmospheric heating rates and radiative fluxes. The performance of the model has been evaluated by comparison with the results of ICRCCM (Intercomparison of radiative codes in climate models). It has been demonstrated that the presented model has a capability to

calculate the solar radiation not only accurately but also economically.

The characteristics of ultraviolet-B radiation (UV-B; 280-320nm) are examined by comparison of relation between the flux at the top of atmosphere and that at the surface. The relation of UV-B is quadratic due to the strong ozone absorption in this band. Also, the dependence of the UV-B radiation on the stratospheric ozone depletion and stratospheric aerosol haze due to volcanic eruption has been tested with various solar zenith angles. The surface UV-B increases as the solar zenith angle increases. The existence of stratospheric aerosols causes an increase in the planetary albedo due to the aerosols' backscattering. The plan etary albedo with aerosols' effect has been increases as the solar zenith angle increases. However, the dependence of planetary albedo on the solar zenith angle is not sensitive. It may be caused by the fact that the aerosols' scattering effect becomes saturated with the relatively long path length in a large solar zenith angle.

Finally, the regional impact of stratospheric aerosols due to volcanic eruption on the intensity of UV-B radiation at the surface has been estimated. A direct effect is that the flux is diminished at the low latitudes, while it is enhanced in the high latitudes by the aerosols' photon trap or twilight effect. In the high latitudes, both aerosols' scattering and ozone absorption have strong and opposite impacts to the surface UV-B radiation. As a result of this cancelation, the maximum increase of UV-B radiation is located at the mid-latitudes during spring season in both hemispheres.

1. Introduction

Recently Herman et al. (1991) and Stolarski et al. (1991) reported the global ozone loss was significant based on the analysis of the revised total ozone mapping spectrometer (TOMS) data from January 1, 1979 to December 31, 1989. Gleason et al. (1993) showed the area-weighted global average ozone amount of 1993 was recorded low compared to that of earlier years. The long-lived chlorofluorocarbons (CFCs), such as CFC-11, CFC-12, CFC-113, CFC-114, and CFC-115, anthropogenic chemicals used in refrigeration, aerosol sprays, foam packing and cleaning solvent, are believed to be a major cause of the stratospheric ozone depletion. Another relatively short natural perturbation of stratospheric ozone layer is volcanic eruption. In particular, the effect of 1991 eruption of Mount Pinatubo in Philippines is one of the greatest on the earth climate in this century, including the acceleration of stratospheric ozone depletion (AGU 1992). The role of stratospheric aerosol haze is to enhance the solar reflection (Harshvardhan 1979). This effect of stratospheric aerosols by volcano is significant within a few months after eruption, and then the signal becomes diminished for up to a few years. Mass and Portmass (1989) reported the maximum volcano induced surface temperature decreases of 0.34℃ over land and 0.14℃ over the ocean in the Northern Hemisphere. Hansen and Lacis (1990) estimated the peak radiative forcing of the Pinatubo is about $4W/m^2$, which exceeds the accumulated radiative forcing due to anthropogenic greenhouse gases added to the atmosphere since the industrial revolution started. The detecting of volcanic signature on climate is, however, not easy because of the inadequate data on aerosols' radiative properties and the large natural climate variabilities (e. g., Robock 1991; Bradely 1988; Angell and Korshover 1983, 1985; Mass and Schneider 1977).

One probable effect of stratospheric aerosols is a change in the amount of ultraviolet radiation reaching the earth's surface. The ultraviolet-B band (UV-B; 280-320nm) is a small fraction of the solar radiation based on spectral solar irradiance data of Labs and Neckel (1970) and Neckel

and Labs (1984). However, this UV-B radiation is of great importance because of the biological and pollutant effects (Jager 1985; Smith 1991). The increased UV-B radiation at the earth's surface may cause an increase of skin cancer cases (Urbach 1969). A recent study conducted by Yale University researchers has established a direct link between UV-B and skin cancer, specifically squamous-cell carcinoma (Brash 1991). This study represents the first time a specific carcinogen (and only this carcinogen) has been implicated in the formation of a human tumor. Other studies have connected UV-B, though not so strongly and unequivocally, with damage to photo-synthesis (Behrenfeld 1989; Tevini and Teramura 1989; Trocine et al. 1981; Lorenzen 1979), particulary in certain crops such as soybean, wheat, and corn (Teramura 1987; Biggs et al. 1988; Eisenstark et al. 1985).

In addition to direct human health and terrestrial (and some aquatic/marine) ecosystem damage through increased UV-B radiation, stratospheric perturbation can also influence these systems through its potential to elevate tropospheric ozone levels. A number of researchers have indicated that alterations in the amount of ozone in the stratosphere and its resultant atmospheric temperature change could lead to significant increases in the amount of ozone in the troposphere. Styles et al. (1987) reported that for each one percent reduction in stratospheric ozone, average tropospheric ozone level will increase by approximately 0.7 to 0.9 percent when averaged over several regions. Tropospheric ozone has been well-established as a major cause of crop and forest damage and also has the ability to impair human health. In fact, ozone in the troposphere is regarded as an air pollutant of greatest current threat to forest and crop health in most of the United States (Smith 1991).

The short-term data of the UV-B fluxes over a limited area can be obtained with a simple radiative transfer model. However, the long-term estimation of the UV-B fluxes with a simple radiative transfer model is not easy because the UV-B fluxes at the earth's surface are influenced by numerous atmospheric conditions, such as clouds, aerosols, and surface albedo (Lubin and Fredrick 1991). In this work, we estimate the seasonal and latitudinal changes of UV-B radiation only for cloud-free sky due to the stratospheric ozone depletion and stratospheric haze by the volcanic eruption with a radiative transfer model.

2. Model description

2.1 Radiative transfer model

The radiative transfer model (RTM) used in this work, summarized in Table 1, is basically the same as that of Oh and Jung (1993) except for the UV-B radiation calculation. For the UV-B radiation we consider two bands - one is a narrow band of 280-320nm and the other is 300nm only. As described in Oh and Jung (1993), the solar radiation is composed of three parts - direct dounward, diffusive downward, and diffusive upward radiations with scattering by air molecules and aerosols and absorption by ozone.

The Rayleigh scattering optical depth is given by

$$\delta_{R,\,i} = \frac{\int_{\lambda_i}^{\lambda_{i+1}} \delta_\lambda \, S_{\infty,\lambda} \, d\lambda}{\int_{\lambda_i}^{\lambda_{i+1}} S_{\infty,\lambda} \, d\lambda} \qquad (1)$$

where

$$\delta_\lambda = r\lambda^{-4} \qquad (2)$$

Table 1. Characteristics of solar and longwave radiation parameterizations.

	process	comments
SOLAR RADIATION		
		Two-stream/delta-Eddington method employing 3 broad spectral intervals (0-0.44μm, 0.44-0.69μm, 0.69-3.85μm)
	Scattering	
	Rayleigh	Ghan (1986)
	Aerosols	
	Gas absorption	
	H_2O	6k-distribution intervals
	CO_2	Fouquart (1988)
	O_3	Lacis and Hansen (1974)
LONGWAVE RADIATION		
		Calculation based on the two-stream formula of the flux equations with parameterized optical depths, Pressure scaling is employed
	Gas absorption	
	H_2O	Chou (1984) and kneizys et al. (1988) 4 broad bands with e-type continuum.
	CO_2	Chou and Peng (1983)
	O_3	Kneizys et al. (1988)
	Trace gases	Donner and Ramanatan (1980). Ramanathan et al. (1985), 10 sub-bands.

and λ is the wavelength of the radiation in μm and $r = 8.8\times10^{-3}$ μm^4 which is given by Ghan (1986) to fit the data in Coakley et al. (1983).

The optical properties of stratospheric aerosols can be evaluated from the Mie theory with information of aerosol size distribution and reflection index which depends on the chemical composition. However, they are assumed in this study as followings; 1) the optical depth of stratospheric aerosols depends on the volcanic scenarios, 2) the single scattering albedo is set to 0.998, 3) the asymmetric factor is set to 0.71, 4) in the stratosphere scattering by air molecules is neglected, however, absorption by ozone and scattering by aerosols are included, and 5) for convenience the surface albedo of the diffusive solar radiation is set to the same value as that of the direct solar radiation.

As shown in Fig. 1, the transmission functions of ozone in the UV-B band have been obtained as in Ghan et al. (1982). When the effective ozone amount is less than 10^{-4} cm -NTP, the layer is transparent for the UV-B radiation. On the other hand, when the effective ozone amount is larger than 10 cm-NTP, the UV-B radiation can not penetrate the layer.

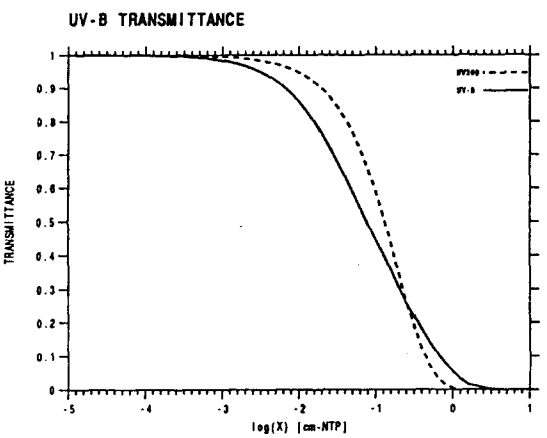

Fig. 1. UV-B transmittance depend on the effective ozone amount.

2.1 Validation of radiative transfer model

The performance of solar radiation model described above is compared with other models reported in the intercomparison of radiative codes in climate models (ICRCCM) (Ellingson and Fouquart 1990) for various sky conditions (57 test cases). In this ICRCCM twenty-four radiation codes including eleven narrow band and thirteen wide band models are intercompared. Table 2 shows the selected cases for the validation of the solar radiation parameterizations, particularly for ozone absorption and scattering.

Table 2. Summary of the cases for the validation of described solar parameterization.

Absorbing only cases

case[1]	atmosphers[2]	gases[3]	Z[4]
19	MLS	all gases $CO_2$300	30°
21	MLS	all gases $CO_2$300	75°
23	TRO	all gases $CO_2$300	30°
25	TRO	all gases $CO_2$300	75°
27	SAW	all gases $CO_2$300	30°
29	SAW	all gases $CO_2$300	75°

Absorbing+Scattering cases (MLS, all gases, CO_2 300ppmv)

case	α_s[5]	Z	case	α_s[5]	Z
31	0.2	30°	32	0.8	30°
33	0.2	75°	34	0.8	75°

1. The case number is the same as in Ellingson and Fouquart (1990).
2. MLS, TRO, and SAW represent midlatitude summer, tropical, and sub-arctic winter atmosphere, respectively.
3. All gases includes H_2O, O_2, O_3, CO_2.
4. Z is the solar zenith angle.
5. α_s is the surface albedo.

2.2.1 Absorbing only cases

Six different absorption only cases, in which the ozone absorbtion is included, are compared with the ICRCCM, ranging from tropical atmospheric profile to mid-latitude summer and sub-arctic winter profiles in McClatchey et al. (1973). Table 3 shows the performance of the described solar radiation parameterization compared to a statistical summary by Ellingson and Fouquart (1990) for both the downward flux (direct radiation+ diffusive radiation) at the surface and the total atmospheric absorption (ABS) defined as

$$ABS = F^{net}_{TOA} - F^{net}_{SFC}, \quad (3)$$

where F^{net}_{TOA} and F^{net}_{SFC} are the net downward solar radiation at the top of atmosphere (TOA) and surface (SFC), respectively.

a) Absorption with all gases cases

Table 3 shows the results of the described solar radiation parameterization for the all gases (H_2O, O_3, O_2, and CO_2) absorption cases. The first line in each case is the statistics of high resolution models, while the second is those of low resolution models or GCM type radiation models. This will be true for all following tests in this study. The statistics show medians of the reported model results, total range of the highest value to the lowest, and standard deviation from the mean of medians. All downward fluxes of the RTM are somewhat underestimated and the differences from the medians are slightly larger than the rms (root-mean-square) differences. Accordingly, the total atmospheric absorptions by the RTM are somewhat larger than medians as shown in Table 3.

Table 3. Summary of the statistical results for absorption with all gases.

Downward flux at the surface

case	median W/m²	range %	rms diff. %	RTM w/m²	diff. %
19	978.1	4.0	1.2		
	985.3	3.5	1.0	967.1	1.9
21	269.3	7.5	2.3		
	271.9	4.6	1.5	261.6	3.8
23	964.7	4.0	1.5		
	977.0	3.1	1.0	956.7	2.1
25	269.6	8.9	2.8		
	269.7	4.8	1.6	257.3	4.6
27	1038.9	5.2	1.5		
	1041.9	3.0	0.9	1030.8	1.1
29	287.8	4.9	1.4		
	288.8	3.9	1.2	284.6	1.5

Total atmospheric absorption

case	median W/m²	range %	rms diff. %	RTM w/m²	diff %
19	212.5	12.8	4.6		
	205.0	17.2	5.1	228.2	11.3
21	84.6	16.8	5.8		
	87.7	15.9	5.2	93.2	14.1
23	223.3	13.2	5.1		
	213.9	16.0	4.9	238.2	11.4
25	84.1	21.3	8.3		
	83.8	15.4	5.4	97.3	16.1
27	149.9	35.3	9.5		
	146.2	25.0	7.5	164.4	12.5
29	66.3	16.6	4.8		
	65.3	17.6	5.9	70.2	7.5

Basically the low resolution models have a tendency to absorb less solar radiation than the high resolution models. The downward (absorbed) fluxes of the low resolution models are larger (smaller) than those of high resolution models, however, the RTM absorbs more solar radiation than the high resolution models. Thus, the differences of the RTM value from medians also exceed the rms differences. In most cases, however, the results of the RTM are located within the rms differences of the high resolution models.

2.2.2 Absorption with all gases cases and Rayleigh scattering

Table 4. shows the results of cases including not only absorption by all gases but also Rayleigh scattering by air molecules. The basic feature mentioned above does not change even with the Rayleigh scattering. The downward fluxes of the low resolution models are larger than those of the high resolution models except for the case of the surface albedo is 0.8 and the solar zenith angle is 30° (case 32). In absorption plus scattering cases the downward fluxes at the surface by the high resolution models are much larger than those by the low resolution models.

Similar to previous results in section 2.2.1, the downward fluxes at the surface of the RTM are somewhat underestimated, while the total atmospheric absorption of the RTM are overestimated. In particular, the differences of the RTM's values from medians are about same size of the rms differences of the downward fluxes and about twice larger than the rms differences of the total absorbed fluxes.

Table 4. Summary of the statistical results for absorption by all gases and Rayleigh scattering.

Downward flux at the surface

case	median W/m²	range %	rms diff. %	RTM w/m²	diff. %
31	942.5	4.3	1.4		
	944.2	4.5	1.5	934.8	1.0
32	985.6	4.1	1.4		
	980.4	3.6	1.4	967.2	1.4
33	234.2	9.7	2.8		
	237.5	5.0	1.7	235.8	0.7
34	245.8	16.9	4.6		
	250.4	8.0	3.3	243.0	3.0

Total atmospheric absorption

case	median W/m²	range %	rms diff. %	RTM w/m²	diff. %
31	209.1	18.0	5.8		
	205.5	9.5	3.8	226.0	10.0
32	248.1	15.0	5.1		
	241.4	25.5	8.9	275.1	14.0
33	85.5	15.3	5.4		
	81.6	11.4	3.8	91.7	12.4
34	92.8	15.9	6.2		
	87.5	18.3	6.1	98.9	13.0

3. Optical characteristics of UV-B radiation

3.1 Relationship of UV-B flux at the top of atmosphere (TOA) and the surface (SFC)

Both total fluxes of solar radiation and UV-B radiation at TOA as well as SFC are calculated with the radiative transfer model described in section 2. The atmospheric conditions used in this study are obtained with inter- or extrapolation from the five basic vertical distributions of major atmospheric components in McClatchey et al. (1973).

To understand the basic optical properties of UV-B compared to the total flux of solar radiation, the radiative fluxes at TOA and SFC are compared and then, the radiative role of each atmospheric composition has been examined. For convenience the Northern Hemisphere has been divided to three parts — low latitude (0°-30°N), middle latitude (30°-60°N), and polar region (60°-90°N). Then, only the middle and polar regions are selected to compare because the stratospheric ozone is not much changed in the low latitude region (Stolarski et al. 1991).

As shown in Fig. 2, the relationships of solar radiation between at TOA and SFC are linear, and the ratios between two fluxes are about 0.75-0.80. In other words, about 75-80 % of the solar radiation at TOA reaches the surface. This is true for all seasons and latitudes. As Shown in Fig. 3, however, the relationships of UV-B radiation at between TOA and SFC are no longer linear differently from the total solar radiation cases. Also, only 10% of the UV-B at TOA reaches the surface. The similar features are observed for other seasons and latitudes.

Table 5 shows the seasonal and regional fitting polynomials for the relation of fluxes at TOA and SFC of both solar radiation and UV-B radiation. As in Table 5, the coefficients of fitting polynomials are not much different from each other for all seasons and regions. This non-linear relation of UV-B is caused by the strong ozone absorption in the UV-B band.

Relation between Total Insolation at TOA and SFC for the region of 30-60N (left) and 60-90N (right)

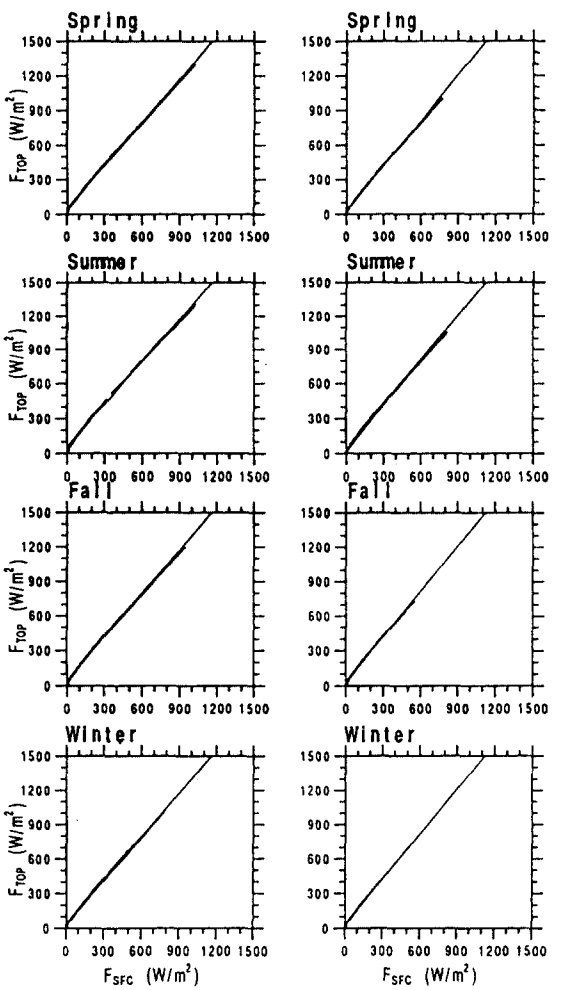

Fig 2. The scatterdiagram for the solar radiation at TOA and SFC. The data have been collected from the results of radiative transfer calculation for one year period. Each dot represents the solar flux at the surface (F_{SFS}) with that at TOA (F_{TOA}). The thin line in each panel is a fitting curve.

Relation between UV-B (280-320nm) at TOA and SFC for the region of 30-60N (left) and 60-90N (right)

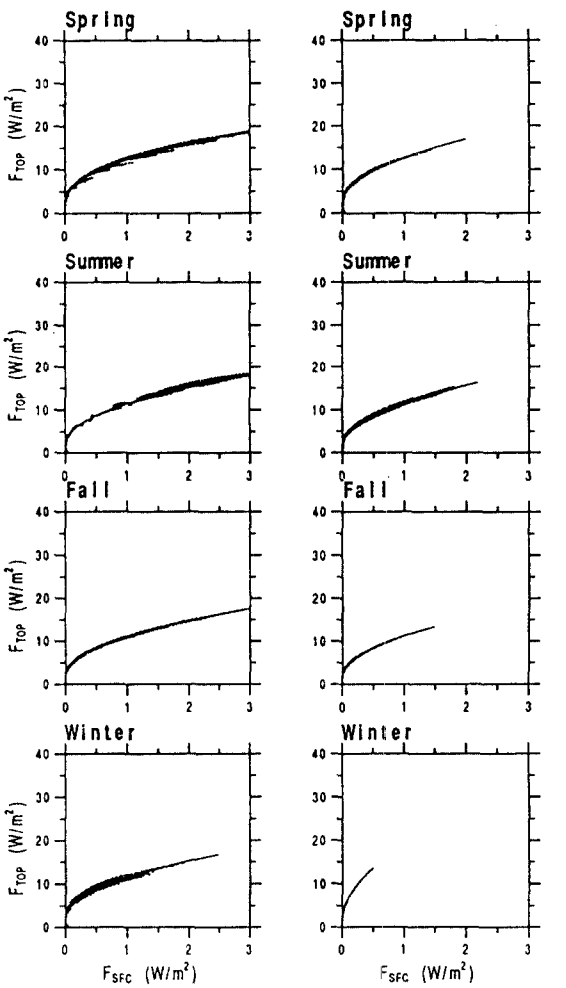

Fig 3. As in Fig. 2 except for UV-B (280-320nm) radiation.

Figs. 4 and 5 are the same as in Figs. 2 and 3 except for ozone absorption, and the curve in each panel of Figs. 2 and 3 is plotted again in Figs. 4 and 5 for comparison. The relation of total solar radiation is linear regardless of whether ozone absorption is included or not. As shown in Fig. 5, however, the relation of UV-B becomes linear by removing ozone absorption. Also the flux at the surface is about 50% of the flux at TOA.

Relation between Total Insolation at TOA and SFC without O_3 effect

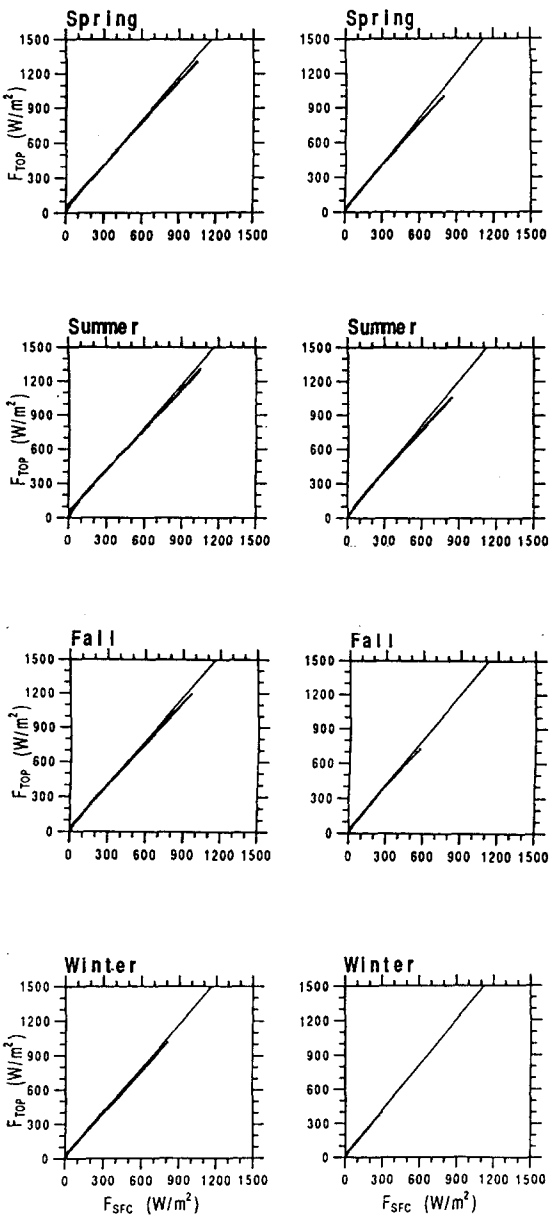

Fig 4. As in Fig. 2 except for the case without ozone.

Relation between UV-B (280-320nm) at TOA and SFC without O_3 effect

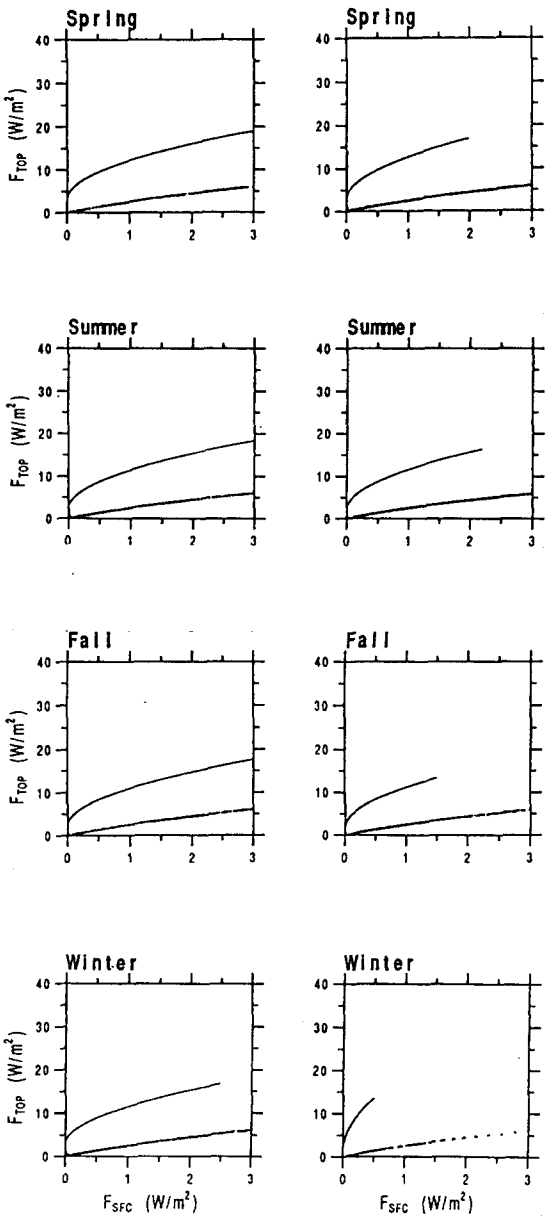

Fig 5. As in Fig. 2 except for UV-B (280-320nm) radiation without ozone.

Figs. 6 and 7 show the results of similar tests above but removing scattering instead of removing ozone absorption to understand the impact of scattering on the nonlinear relation between the UV-B fluxes at TOA and SFC. As shown in Figs. 6 and 7, the results are quite similar to the cases with scattering in Figs. 2 and 3 except that the surface fluxes are somewhat enhanced. Therefore, the quadratic relation of fluxes between at TOA and SFC is mainly due to the strong ozone absorption in the UV-B band.

Relation between Total Insolation at TOA and SFC without scattering

Relation between UV-B(280-320nm) at TOA and SFC without scattering

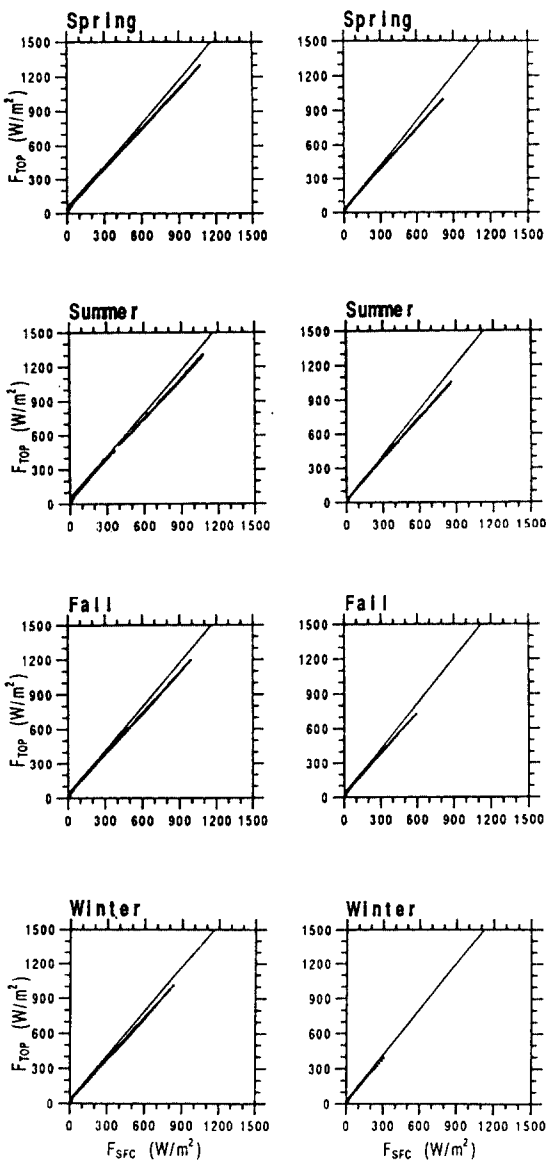

Fig 6. As in Fig. 2 except for the case without scattering.

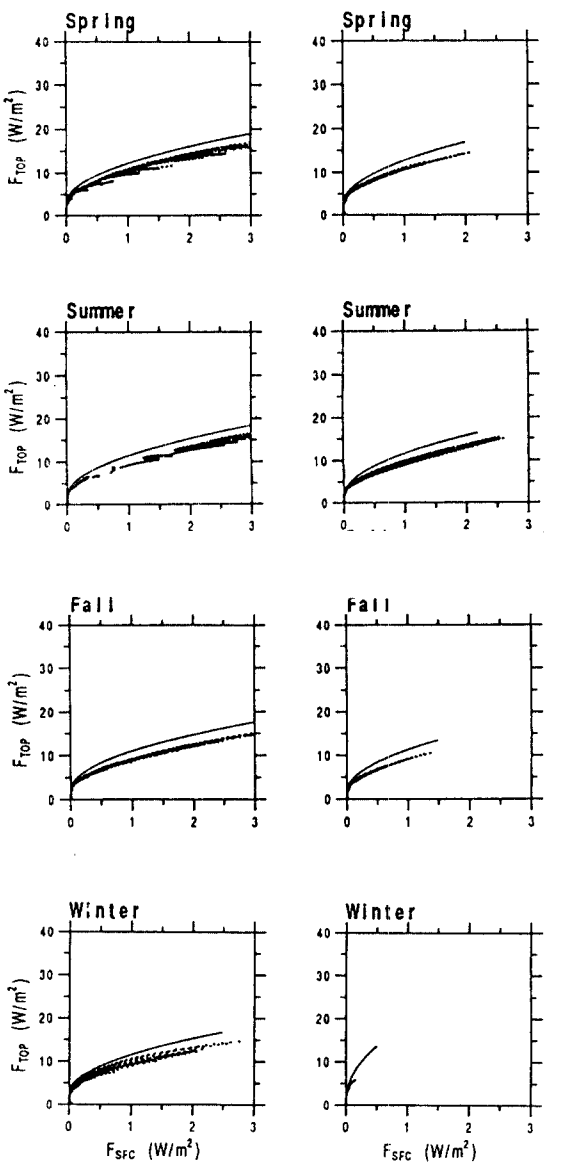

Fig 7. As in Fig. 2 except for UV-B (280-320nm) radiation without scattering.

Table 5. Fitting polynomials for the relation of fluxes at TOA and SFC.

band	Fullband		UV-B(280-320nm) band		
curve	$F_{SFC} = C_1 \times F_{TOA} + C_2$		$F_{SFC} = C_1 \times F_{TOA}^2 + C_2 \times F_{TOA} + C_3$		
coeff.	C_1	C_2	C_1	C_2	C_3
30-60N Region					
Spring	0.813	-45.27	1.19e-2	-7.30e-2	1.16e-1
Summer	0.813	-44.05	1.12e-2	-4.45e-2	3.13e-2
Fall	0.801	-31.08	1.20e-2	-4.39e-2	3.13e-2
Winter	0.792	-28.42	1.22e-2	-5.90e-2	6.33e-2
60-90N Region					
Spring	0.768	-23.8	9.54e-2	-4.68e-2	4.93e-2
Summer	0.748	-7.34	1.02e-2	-3.39e-2	2.48e-2
Fall	0.790	29.6	1.06e-2	-3.20e-2	2.17e-2
Winter	0.764	-21.6	3.14e-3	-6.17e-3	2.96e-3

3.2 Dependence of UV-B flux on the ozone depletion, solar zenith angle and surface albedo

The integrated optical characteristics of UV-B radiation for various locations and seasons have been presented in the previous section. The UV-B radiation at the surface can be largely changed by various atmospheric conditions, such as total ozone amount, aerosol amount and solar zenith angles, Particularly, it has been known that the increase of surface UV-B radiation due to 1% stratospheric ozone depletion is about 2%, and it may cause about 4% increase of skin cancer cases.

Fig. 8 shows the dependence of surface UV-B flux on the stratospheric ozone depletion and solar zenith angle. The left panels are for the cases of 300nm, while the right panels are for the broad UV-B band. The upper, middle and lower panels are, respectively, for the cases of surface albedo is 0.1, 0.2, and 0.4. The atmospheric condition is assumed to be the mid-latitude summer case of McClatchey et al. (1973).

In most cases, the surface UV-B radiation becomes larger as the solar zenith angle becomes larger. Particularly the case of solar zenith angle is larger than 50°, it becomes more notable. For example, 20% of stratospheric ozone depletion causes more than 100% increase of surface UV-B radiation for the 300nm and 30% increase for the 280-320nm band when the solar zenith angle is larger than 70°.

The impact of UV-B radiation on the surface ecosystem depends on the reflected UV-B radiation as well as the downward UV-B radiation near the surface. Thus, the surface albedo can be an important factor to estimating the impacts of UV-B radiation on the surface ecosystem. However, the change of surface UV-B radiation with different surface albedos is not notable.

⊿UV-B at SFC due to St. O_3 Depletion & Tr. O_3 Increase

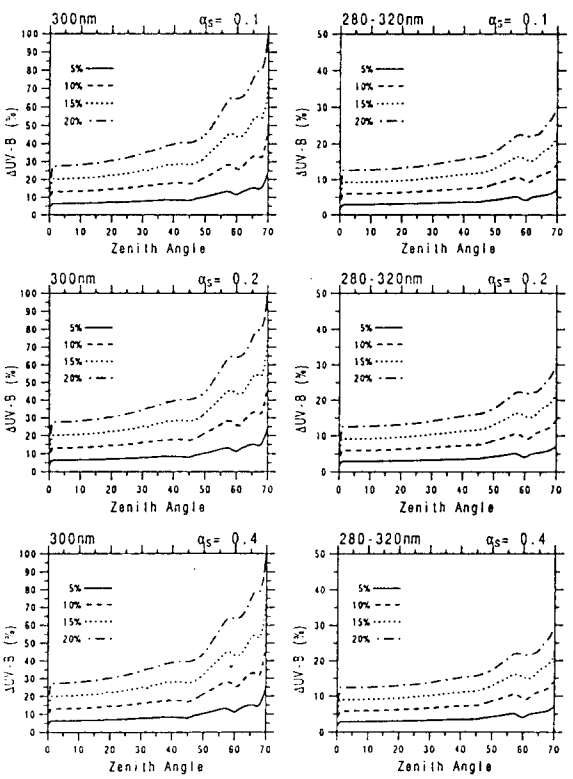

Fig 8. Dependence of surface UV-B radiation on the solar zenith angle. The left panels are for the UV-B change of 300nm, while the right panels are for 280-320nm. The upper, middle and lower panels are for the case of the surface albedo (α_s) is 0.1, 0.2, and 0.4, respectively. In each panel, the solid, dashed, dotted, hybrid lines, respectively, represent the cases of control, 5%, 10%, and 20% stratospheric ozone depletion.

3.3 Dependence of UV-B flux on the optical depth of aerosols and solar zenith angles

The existence of stratospheric aerosols can diminish the radiation in the troposphere. Halpert et al. (1993) estimated 0.1 increase of stratospheric aerosol optical depth may cause 1% increase of planetary albedo in a global mean sense. However, the increase of planetary albedo due to the increase of aerosol optical depth may depend on the solar zenith angle. The upper panel of Fig. 9 shows that the planetary albedo increases monotonically as the solar zenith angle grows. And the increase of albedo becomes more significant, when the zenith angle is larger than 50°. For the other cares, however, the albedo increases about 2.5% for every 0.1 aerosol optical depth increse.

This is only applied to the case of cloud-free sky. For the cloudy sky the effects of aerosols on the planetary albedo change may not be significant due to the relative thick cloud's optical depth. If the global-averaged cloudiness is assumed as 60% and no albedo change is assumed in the cloudy sky by aerosol optical depth change, the estimation of 2.5% for the clear sky can match to Halpert et al.'s 1% increase of planetary albedo with every 0.1 aerosol optical depth increase.

In the 300nm cases presented in the middle panel of Fig. 9, however, the solar zenith angle is no longer an important factor. The increase of albedo is about 0.3% for each 0.1 increase of optical depth. Different from the total solar radiation, the albedo change of the broad UV-B band becomes diminished as the solar zenith angles increases. This low sensitivity of UV-B radiation at the high solar zenith angle to the change of aerosol optical depth is caused by the fact that aerosol scattering effect is almost saturated due to the relatively long path length in this range of solar zenith angles.

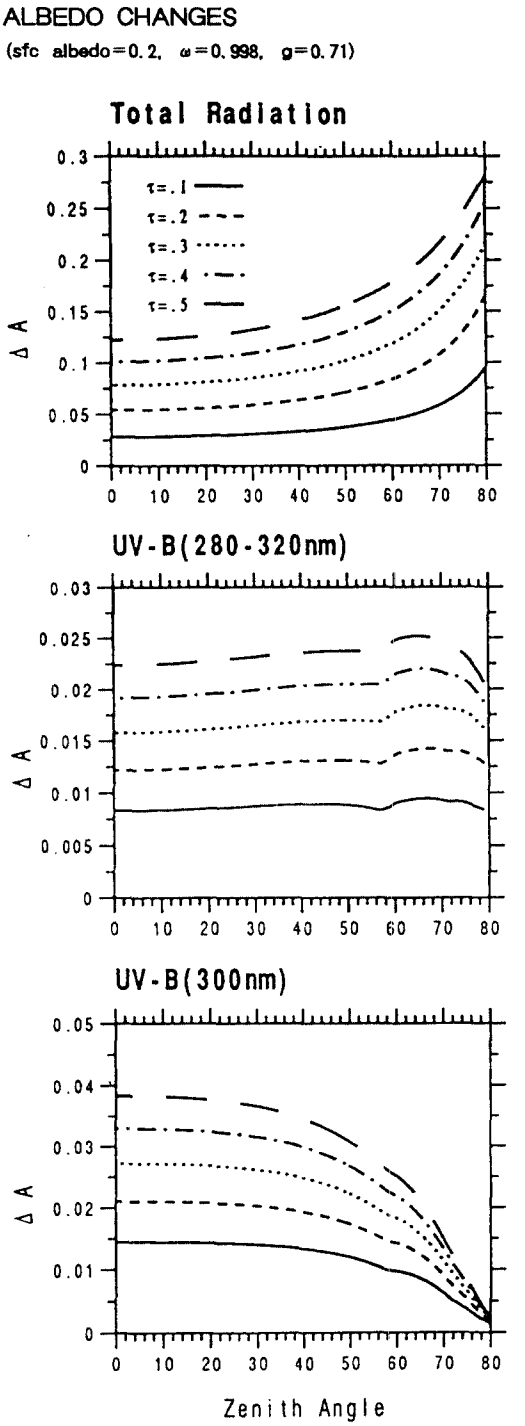

Fig 9. Planetary albedo change with various solar zenith angle. The upper, middle and lower panels are for the full spectrum solar radiation, broad UV-B band (280-320nm), and 300nm, respectively.

4. Impact of the volcanic eruption on the surface UV-B radiation

The volcanic eruption may introduce a huge amount of aerosols into the lower stratosphere. DeFoor et al. (1992) reported the time series of the non-Rayleigh backscatter values and volcanic explosive index (Simkin et al. 1987) of the major volcanic eruptions in the equatorial and Northern Hemisphere based on the Lidar measurement at Mauna Loa Observatory. The El Chichon of 1981 and Pinatubo of 1991 are the most distinguishable volcanic eruptions since 1981. Michelangeli et al. (1992) estimated the stratospheric volcanic aerosols by El Chichon volcano, of which the optical depth was about 0.25 at 6000-7000Å as measured at 20°N latitude (DeLuisi et al. 1983), increase the surface UV-B flux as much as 45% at 2900Å

To understand the impact of volcanic eruption on the surface UV-B radiation, two scenarios are considered. One is the volcanic eruption at the low latitude (15°N), and the other is at the high latitude (60°N) in the Northern Hemisphere as shown in the upper panels of Fig. 10. The aerosol optical depth is assumed as 0.3 at the latitudes near the eruption, and then reduced gradually for the farther latitudes from volcano. For computation the atmospheric condition is assumed as the interpolated values with respect to time and location from the vertical distributions of ozone, temperature and water vapor of McClatchey et al.'s (1973) five basic atmospheric conditions - tropics mid-latitude summer, mid-latitude winter, sub-arctic summer, and sub-arctic winter. However, the monthly mean total ozone amount is obtained from the TOMS daily measurement data (Bowman 1988). The surface albedo remains fixed for all latitudes and seasons.

The middle panels of Fig. 10 show the changes of daytime mean UV-B radiation at the surface with a contour interval of 10mW/㎡. The left panel is for the low latitude volcano case, while the right panel is for the high latitude case. The general features of stratospheric aerosol effect are as follows; 1) the surface UV-B fluxes are diminished at the low latitudes due to aerosols' backscattering, however, those are enhanced at the high latitudes in both hemispheres, 2) the increase of surface UV-B radiation due to the stratospheric aerosols is largest at the middle latitudes during winter season in both hemispheres, 3) both panels show the impact of volcanos on the surface UV-B radiation is less significant during summer, and 4) the UV-B fluxes decrease significantly during spring and fall at the low latitudes.

These features are not much changed for the case of either low latitude volcanic eruption or high latitude eruption. The only difference of high latitude eruption is that the change of UV-B radiation is much larger in the Northern Hemisphere than that in the Southern Hemisphere because of uneven distribution of aerosols in both hemispheres as shown in the upper panels of Fig. 10. In terms of percentage, as shown in the lower panels of Fig. 10, the largest increase of UV-B radiation is located at high latitudes in both hemispheres due to the relatively small amount of UV-B fluxes at this region compared to those in the low latitudes.

This increase of surface UV-B fluxes at the high latitudes is supported by Michelangeli et al.'s (1989, 1992) photon trapping theory and Davie's (1993) twilight effect that the surface UV-B radiation can be substantially increased by the stratospheric aerosols' scattering when the solar zenith angle is large at the high latitudes. It is different from the total spectrum solar radiation case in which the scattering by the volcanic aerosols results in the more reflected radiation to space as shown in the upper panel of Fig. 9 and the diminished surface radiation as a result of increase of aerosols' backscattering.

Thus, the volcanic eruption may cause a significant increase of UV-B radiation which is harmful to human and our ecosystem. Also, it can perturb the photochemical processes of stratosphere, in particular a reduction of stratospheric ozone. Halpert et al. (1993) reported the Mount Pinatubo of Philippines is responsible for recent extreme low values of observed total ozone amount in 1991 and 1992 (Gleason et al. 1993).

Schematic Optical Depth Distribution due to Volcanos

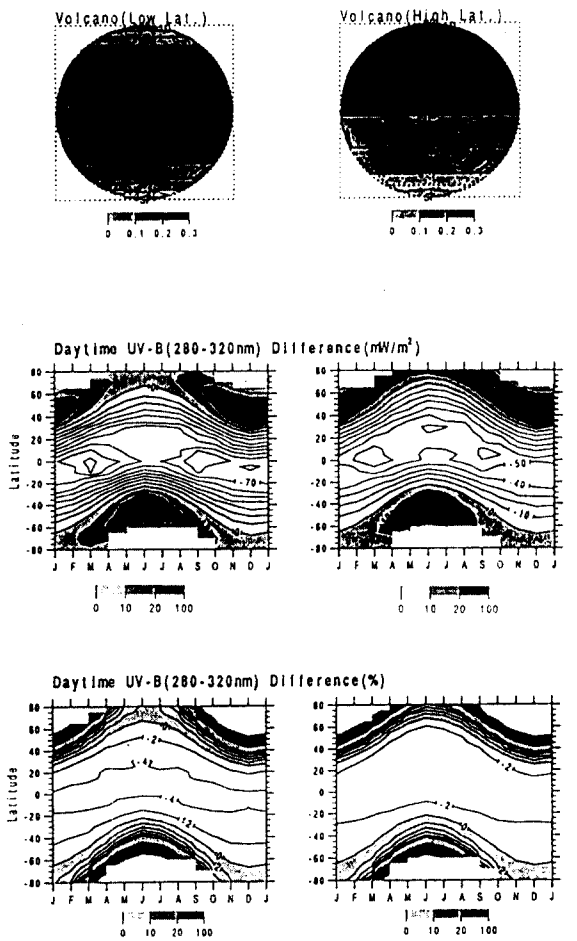

Fig 10. Volcnaic optical depth distribution (upper panels) and the surface UV-B radiation changes in a unit of mW/m^2 (middle panel) and percentage (lower panel). The left panels are for the low latitude volcanos while the right panels are for high latitude volcanos in the Northern Hemisphere.

5. Summary and conclusion

The performance of RTM used in this study has been demonstrated by comparison with the results of other codes reported to ICRCCM (Ellingson and Forquart 1990). The presented RTM belongs to a category of low resolution models, however, the calculated fluxes are much closer to those of high resolution models in most ICRCCM test cases. Thus, the presented RTM can be used for accurate and economic calculation of the solar radiation transfer through the atmosphere and at the TOA as well as at the surface.

The radiative fluxes at TOA and SFC have been calculated to understand the basic optical properties of UV-B compared to the total flux of solar radiation. 75-80% of solar radiation at TOA reaches the surface and the relationship between the solar radiation at TOA and SFC is linear, while only 10% of UV-B flux at TOA reaches the surface and the relationship is quadratic mainly due to the strong ozone absorption in the UV-B band (280-320nm). The stratospheric aerosols do not change the feature of relation between the fluxes at TOA and SFC, but do somewhat enhance the surface flux.

The change of surface UV-B radiation with stratospheric ozone depletion becomes more significant as the solar zenith angle becomes larger. Particularly, when the solar zenith angle is larger than 50°, it becomes more notable. The existence of stratospheric aerosols increases the planetary albedo due to backscattering by aerosols. The planetary albedo for full spectrum solar radiation increases monotonically as the solar zenith angle grows. However, the albedo change of the broad UV-B band becomes diminished as the solar zenith angle increases. This diminishing of UV-B albedo change may be caused from the fact the aerosol scattering effect is almost saturated by the relatively long path length in this range of solar zenith angles.

One of most important direct impacts of volcanic eruption on the surface UV-B radiation is that the surface UV-B fluxes are diminished at the low latitudes, however, those are enhanced at the high latitudes due to the aerosols' photon trap or twilight effect. This increase of surface UV-B radiation at high latitudes can be more significant by considering of the indirect effect of stratospheric aerosols which induces an enhancement of the stratospheric photochemical processes related to ozone reduction.

In high latitudes, both aerosols' scattering and ozone abrorption are strong. As a result of this cancelation between scattering and absorption effects, the maximum change appears at the mid-latitudes during spring season in both hemispheres.

Acknowledgements

We thank Dr. H.-K. Cho and J.-J. Baik for their review and fruitful discussion. Also, we are grateful to S.-N. Oh for his suggestion. This research was supported by the project-"Development on Coupled Ocean/Atmosphere GCM" of "Research and Development on Technology for Global Environmental Monitoring and Climate Change Prediction", which is one of "G-7 Projects" of the Korea Environment Administration.

References

AGU, 1992 : Volcanism and climate change. AGU special report, American Geophysical Union, Washington. D. C., 27pp.

Angell, J. K., and J. Korshover, 1983 : Comparison of stratospheric warmings following Agung and El Chichon. *Mon. Wea. Rev.*, **111**, 2129-2135.

Angell, J. K., and J. Korshover, 1985 : Surface temperature changes following the six major volcanic episodes between 1780 and 1980. *J. Clim. Appl. Meteor*, **24**, 937-951

Behrenfeld, M., 1989 : Primary productivity in the southeast Pacific : effects of enhanced ultraviolet-B radiation. M. S. Thesis, Department of general science, Oregon State University, Corvallis, OR, 37pp.

Biggs, R. H., S. A. Hamilton, and B. A. McCarl, 1988 : The benefits of pollution control : the case of ozone and U. S. agriculture. *Am, J. Agricultural Economics*, **68**, 886-893.

Bowman, K. P., 1988 : Global trends in total ozone. *Science*, 239, 48-50

Bradley, R. S., 1988 : The explosive volcanic eruption signal in Northern Hemisphere continental temperature records. , *Climate Change*, **12**, 221-243.

Brash, D. E., 1991 : The proceedings of national academy of sciences.

Chou, M.-D., 1984 : Broadband water vapor transmission functions for atmospheric IR flux computation. *J. Atmos. Sci.*, **41**, 1775-1778

Chou, M.-D., and L. Peng, 1983 : A parameterization of the absorption in 15μm CO_2 spectral region with application to climate sensitivity studies. *J. Atmos. Sci.*, **40**, 2183-2192.

Coakley, J. A., Jr., R. D. Cess, and F. B. Yurevich, 1983 : The effect of tropospheric aerosols on the Earth's radiation budget : A parameterization for climate models. *J. Atmos. Sci.*, **40**, 116-138.

Davies, R., 1993 : Increased transmission of the ultraviolet radiation to the surface due to stratospheric scattering. *J. Geophys. Res.*, 98, 7251-7253

DeFoor, T. E., E. Robinson, and S. Ryan, 1992 : Early lidar observations of the June 1991 Pinatubo eruption plume at Mauna Loa Observatory, Hawaii. *Geophys. Res. Lett.*, **19**, 187-190.

DeLuisi, J. J., E. G. Dutton, K. L. Coulson, T. E. DeFoor, and B. G. Mendonca, 1983 : On the some radiative features of the El Chichon volcanic stratospheric dust cloud and a cloud of unknown origin

observed at Mauua Loa, *J. Geophys. Res.*, 88, 6769-6772.

Donner, L., and V. Ramanathan, 1980 : Methane and Nitrous Oxide : Their effects on the terrestrial climate. *J. Atmos. Sci.*, 37, 119-124

Eisenstark, A., G. H. Perrot, G. Ulmer, and C. D. Miles, 1985 : Enhanced UV-B irradiation (190-320) of Corn (Zea mays L.) I. Effects on growth and yield. Final project report, EPA Report 808132-10, Corvallis, Oregon.

Ellingson, R, G., and Y. Fouquart, 1990 : Radiation and Climate : Intercomparison of Radiation Codes in Climate Models (ICRCCM). Report of workshop, WCRP-39, WMO/TD-No. 371, 36pp.

Fouquart, Y., 1988 : Radiative transfer in climate modeling. In *Physically-Based Modelling and Simulation of Climate and Climate Change*, M. E. Schlesinger (ed.), NATO Advanced Study Institute Series, Kluwer, Dordrecht, pp. 223-283.

Ghan, S. J., 1986 : Personal communication.

Ghan, S. J., J. W. Lingaas, M. E. Schlesinger, R. L. Mobley and W. L. Gates, 1982 : A documentation of the OSU two-level atmospheric general circulation model. Report No. 35, Climatic Research Institute, Oregon State University, Corvallis, OR, 395 pp.

Gleason, J, F., P. D. Bhartia, J. R. Herman, R. McPeters, P. Newman, R. S. Stolarski, L. Flinn, G. Labow, D. Larko, C. Seftor, C. Wellemeyer, W. D. Komhyr, A. J. Miller, and W. Planet, 1993 : Record low global ozone in 1992. *Scinece*, 260 523-526

Halpert, M. S., C. F. Ropelewski, T. R. Karl, J. K. Angell, L. L. Stowe, R. R. Heim, Jr., A. J. Miller, and D. R. Rodenhuis, 1993 : 1992 brings return to moderate global temperatures. *EOS*, 74, 433-439.

Hansen, J., and A. Lacis, 1990 : Sun and dust versus greenhouse gases : An assessment of their relative roles in global climate change. *Nature*, 346, 713-718.

Harshvardhan, 1979 : Perturbation of the zonal radiation balance by a stratospheric aerosol layer. *J. Atmos. Sci.*, 36, 1274-1285.

Herman, J. R., R. McPeters, R. Stolarski, D. Larko, and R. Hudson, 1991 : Global average ozone change from November 1978 to May 1990. *J. Geophys. Res.*, 96, 17, 297-17, 305.

Jager, J., 1985 : *Solar-UV actions on living cells.* Praeger Publishers, New York, N. Y., 202pp.

Kneizys, F. X., E. P. Shettle, L. W. Abreu, Chetwynd, G. P. Anderson, W. O. Gallery, J. H., Ir., A. Selby, and S. A. Clough, 1988 : Users Guides to LOWTRAN 7. Potical Physics Div., 7670, Hanscom AFB, Bedford, MA, 137pp.

Labs, D., and H. Neckel, 1970 : Transformation of the absolute solar radiation data into the "International Practical Temperature Scale of 1968." *Solar Physics*, 15, 79-87.

Lacis, A. A., and J. E. Hansen, 1974 : A parameterization for the absorption of solar radiation in the earth's atmosphere. *J. Atmos. Sci.*, 31, 118-133.

Lorenzen, C. J., 1979 : Ultraviolet radiation and photoplankton photosynthesis. *Limmol. Oceanogr.*, 24 (6), 1117-1120.

Lubin, D., and J. E. Frederick, 1991 : The ultraviolet radiation environment of the Antarctic peninsula : The role of ozone and cloud cover. *J. Appl. Meteor.*, 30, 478-493.

McClatchey, R. A., R. W. Fenn, J. E. A. Selby, J. S. Garing, and F. E. Volz, 1973 : *Optical properties of the atmosphere.* AFCRL-70-0527, Air Force Cambridge Research Laboratories, Bedford, MA, pp85.

Mass, C. F., and D. A. Portman, 1989 : Major volcanic eruptions and climate : A critical evaluation. *J. Climate*, 2, 566-593.

Mass, C. F., and S. H. Schneider, 1977 : Statistical evidence on the influence of sunspots and volcanic dust on long term temperature trends. *J. Atmos. Si.*, 34, 1995-

2004.

Michelangeli, D. V., M. Allen, and Y. L. Yung, 1989 : The effect of El Chichon volcanic aerosols on the chemistry of the stratosphere through radiative coupling. Eluszkiewicz, 1993 : Enhancement of atmospheric radiation by an aerosol layer. *J. Geophys. Res.*, 94. 18, 429-18, 443.

Michelangeli, D. V., M. Allen, Y. L. Yung, R.-L. Shia, D. Crisp, and Eluszkiewicz, 1993 : Enhancement of atmospheric radiation by an aerosol layer. *J. Geophys. Res.*, 97, 865-874.

Neckel, H., and D. Labs, 1984 : The solar radiation between 3, 300 and 12, 500 A. *Solar Physics*, 90, 205-258.

Oh, J. -H., and J. -H. Jung, 1993 : A comparison of radiative forcings of atmospheric gases on vertical temperature distribution (to be submitted to J. Kor. Meteor. Soc.).

Ramanathan, V., H. B. Singh, R. J. Cicerone, and J. T. Kiehl, 1985 : Trace gas trends and their potential role in climate change. *J. Geophys. Res.*, 90, 5547-5566.

Robock, A., 1991 : The volcanic contribution to climate change of the past 100 years. In *Greenhouse-gas-induced climatic change : A critical appraisal of simulations and observations* Ed. M. E. Schlesinger, Elsevier Science Publishers B. V., Amsterdam, Netherlands, 429-443.

Simkin, T., L. Seibert, L. McClelland, D. Briege, C. Newhall, and J. H. Latter, 1987 : *Volcanos of the world, Supplement.* Smithsonian Institution, Washington, D. C.

Smith, W. H., 1991 : Air pollution and forest damage. *Chem. Eng. News*, 69, 30-43.

Styles, K. R., M. W. Gery, and G. Z. Whitten, 1987 : Assessment od existing tropospheric ultraviolet radiation data and the effects of its increase on ozone formation in the troposphere. System Apllication Inc., Work in progress for the National Park Service, Denver, Co.

Stolarski, R. S., P. Bloomfield, R. D. McPeters and J. R. Herman, 1991 : Total ozone trends deduced from Nimbus 7 TOMS data. *Geophys. Res. Letters*, 18, 1015-1018.

Teramura, A. H., 1987 : Current understanding of the effects of increased levels of solar ultraviolet radiation to crops and natural plant ecosystems. Testmony before the U. S. Senate.

Tevini, M., and A. H. Teramura, 1989 : UV-B effects on terrestrial plants. *Photochem Photobilolo.*, 50, 479-487.

Trocine, R. P.. J. D. Rice, and G. N. Wells, 1981 : Inhibition of seagrass photosynthesis by ultraviolet-B radiation. *Plant Physiol.*, 68, 74-81.

Urbach, F., 1969 : *The biological effects of ultraviolet radiation*, Pergamon, New York.